Biochimica et Biophysica Acta 1827 (2013) 19–29

Contents lists available at SciVerse ScienceDirect

Biochimica et Biophysica Acta

journal homepage: www.elsevier.com/locate/bbabio

'Domino' systems biology and the 'A' of ATP

Malkhey Verma [a], Maksim Zakhartsev [b], Matthias Reuss [b], Hans V. Westerhoff [a,c,d,*]

[a] Manchester Centre for Integrative Systems Biology, Manchester Institute of Biotechnology, The University of Manchester, Manchester, UK
[b] Institute for Biochemical Engineering (IBVT), University of Stuttgart, 70569 Stuttgart, Germany
[c] Netherlands Institute for Systems Biology, Molecular Cell Physiology, VU University Amsterdam, Netherlands
[d] Synthetic and Systems Biology, The University of Amsterdam, Netherlands

ARTICLE INFO

Article history:
Received 6 July 2012
Received in revised form 17 September 2012
Accepted 23 September 2012
Available online 29 September 2012

Keywords:
Domino systems biology
Domino process
Glycolysis
Adenine nucleotide
IMP salvage
Saccharomyces cerevisiae

ABSTRACT

We develop a strategic 'domino' approach that starts with one key feature of cell function and the main process providing for it, and then adds additional processes and components only as necessary to explain provoked experimental observations. The approach is here applied to the energy metabolism of yeast in a glucose limited chemostat, subjected to a sudden increase in glucose. The puzzles addressed include (i) the lack of increase in Adenosine triphosphate (ATP) upon glucose addition, (ii) the lack of increase in Adenosine diphosphate (ADP) when ATP is hydrolyzed, and (iii) the rapid disappearance of the 'A' (adenine) moiety of ATP. Neither the incorporation of nucleotides into new biomass, nor steady de novo synthesis of Adenosine monophosphate (AMP) explains. Cycling of the 'A' moiety accelerates when the cell's energy state is endangered, another essential domino among the seven required for understanding of the experimental observations. This new domino analysis shows how strategic experimental design and observations in tandem with theory and modeling may identify and resolve important paradoxes. It also highlights the hitherto unexpected role of the 'A' component of ATP.

1. Introduction

Systems biology has the ambition to reveal how and where interactions are essential for biological function. So-called top–down systems biology assesses the dynamic behavior of components in the functioning biological system experimentally. Correlations that persist under a variety of conditions then lead to empirical relationships between the components. By projection onto the genome this may suggest hitherto unknown interactions. A second approach, called bottom–up systems biology starts from the molecular components and their experimentally established interactive properties and then examines by computer modeling to which functional properties these interactions may lead. By then extending this approach to more and more components, the approach expects ultimately to achieve an understanding of the entire system. A third approach has been called 'middle-out' systems biology [1,2]. It starts at some point in between molecular components and entire system, and then examines how at that level interactions produce functional dynamics.

The approaches have a problem in common. This is the immense complexity of even the smallest living systems. Taking the latter as quasi-autonomous systems that are able to sustain themselves in principle indefinitely, in the presence of continuous damage being inflicted upon them by their environment, this complexity has been shown to exceed 300 interacting genes and their products and many more for yeast [3–7]. Removal of any of these makes the organism nonviable. This contention is supported by an estimate of more than 150 processes needed together for life to be sustainable [8]. Consequently, the bottom–up approach would need to take hundreds of molecular processes into account at the same time, and the top–down approach would need to measure the effect of hundreds of independent perturbations for the system to become identifiable in terms of its components. The middle-out strategy would have to be repeated at a multitude of 'intermediate' levels, or combined with bottom–up or top–down systems biology, to enable understanding the level that is being studied fully: some of the regulatory loops controlling the phenomena studied will run through lower or higher levels of organization.

In practice, the three approaches are exercised on systems of reduced complexity, or with a reduced number of perturbations. Most bottom–up systems biology is still restricted to specific parts of the metabolic map of the cell (e.g. glycolysis) or to a specific regulatory structure (e.g. the MAP kinase signaling pathway). In vivo, however, the different cellular sub-systems integrate to form the complete living organism such as a yeast cell. Regulation of a reaction rate in a metabolic pathway by a metabolite in that same pathway may involve the activation of a transcription factor for the gene encoding the enzyme that catalyzes the reaction rate, thereby involving pathways at different levels in the cellular hierarchy [9]. Likewise, in a

* Corresponding author at: Centre for Integrative Systems Biology, Manchester Institute of Biotechnology, The University of Manchester, Manchester-M1 7DN, UK. Tel.: +44 161 306 4407; fax: +44 161 306 4556.
E-mail address: Hans.Westerhoff@manchester.ac.uk (H.V. Westerhoff).

0005-2728/$ – see front matter.
http://dx.doi.org/10.1016/j.bbabio.2012.09.014

gene regulatory network, the regulation of a gene may govern the transcription of part of a different chromosome by encoding a protein that is a transcription factor of the latter. Understanding of even a single, apparently local function of the genome, may involve multiple other parts of that genome: Systems biology requires integrated kinetic models of the whole organism.

For top–down systems biology the first few principal components emerge in a deconvolution of the dynamics, where amplitude of change is supposed to square with importance for function. However, also here the problem of connectivity applies; the total number of principal components might well equal the number of components, if it were not for the experimental noise to make this unobservable: Intracellular networks appear scale-free and are highly connective [10–13]. Strictly speaking therefore, neither bottom–up, nor top–down, nor middle-out systems biology can succeed in elucidating cell function until they are complete in the sense of taking the dynamic functioning of all genes and gene products of an organism into account.

Intuitively, this seems too pessimistic. For sure, certain genes must be less important than others. After all, the control exercised by most genes on cellular fluxes should be small [14,15], and there is substantial redundancy in genetic networks, as evidenced by the many homozygous deletions that are 'silent' in terms of growth rate (although perhaps not in terms of metabolome [16]). There should be a way therefore to focus on the more important functions and on the processes that are most important for these. Subsequently one may then focus on the second most important function, etcetera.

Here we describe a new strategy for systems biology that attempts to do this systematically. We call the approach 'domino systems biology'. Rather than with all molecular components of the systems, this strategy starts with one of the essential functions of life and identifies the major process and the major cellular monitor of that function. These are the two parts of the first 'domino'. By integrating progressive experimentation with modeling, the strategy examines if process and monitor suffice for explaining the observed functioning. When it begins to fail to do so, additional dominoes (processes or monitors) are examined in terms of their ability to restore correspondence between model and experimentation. The first one that is able to do so is then assimilated into the model and the procedure is iterated.

Of biological functions that contribute to the fitness of species, we shall target growth and what is essential for it. In view of the richness of the (bio)chemistry of most species, our domino systems biology may begin with the commodities that cannot be created by chemical processes, following the sequence (Gibbs free) energy, total carbon, total redox (electrons available for reduction–oxidation reactions), total nitrogen, total phosphorous and total sulfur, and then the cofactors and vitamins. We here start with the first of these, and identify the main commoditie(s) representing it and the main process synthesizing that commodity. We then follow the domino strategy described above. The strategy will lead us from ATP and glycolysis to pyruvate, AMP and the nucleotide salvage pathways, producing understanding of the importance of various cellular processes for cellular energetics and growth.

2. Materials and methods

2.1. Model development: domino systems biology

Domino systems biology is a modular approach which begins with a central module and adds dominating biological phenomena as a sequence of modules. The domino method has the additional property that each module is characterized by one or more inputs and one or more outputs. The latter either corresponds to an output of the system as a whole or is identical to the input of a next module. Consequently, modules constitute chains that run from a system input to a system output. The various modules in the model are as follows:

2.1.1. Glycolysis domino

In our first step in the domino approach, glycolysis was taken as a single reaction starting from one glucose molecule and leading to two ATP molecules (Supplementary material Fig. S1):

$$Glucose + 2ADP \rightarrow 2ATP. \quad (1)$$

The rate expression is shown by Eq. (2).

$$\nu^{Gly} = V^{Gly}_{\max} \cdot \left(\frac{Glc \cdot ADP}{K_{mGlyGlc} \cdot K_{mGlyADP} \cdot \left(1 + \frac{Glc}{K_{mGlyGlc}} + \frac{ADP}{K_{mGlyADP}} + \frac{Glc \cdot ADP}{K_{mGlyGlc} \cdot K_{mGlyADP}}\right)} \right). \quad (2)$$

The parameter $K_{mGlyGlc}$, $K_{mGlyADP}$ values used were 0.08 and 0.53 mM respectively, adopted from Teusink model [17]. $V^{Gly}_{\max}$ was calculated to be equal to 226.33 mM/min by fitting the glycolysis flux equal to Teusink model in glucose rich condition (50 mM extracellular glucose) by keeping *Glc* and *ADP* concentrations equal to steady state concentrations in Teusink model 0.098 and 1.29 mM, respectively. This corresponded to our first glycolysis domino with input glucose and output ATP (the left-hand domino in Supplementary Fig. S1).

2.1.1.1. Upper glycolysis domino. As an alternative to the above glycolysis domino, glycolysis was modeled as the integration of three reactions. One started from glucose and two *ATP* and led to fructose-1,6-bisphosphate (*FbP*) and two *ADP* molecules, and was called the 'upper glycolysis domino':

$$Glucose + 2ATP \rightarrow FbP + 2ADP \quad (3)$$

$$\nu^{R1} = V^{R1}_{\max} \cdot \left(\frac{(Glc \cdot ATP)}{K_{mR1Glc} \cdot K_{mR1ATP} \cdot \left(1 + \frac{Glc}{K_{mR1Glc}} + \frac{ATP}{K_{mR1ATP}}\right)} \right). \quad (4)$$

Parameter values K_{mR1Glc}, K_{mR1ATP} were taken as 0.08 and 0.15 mM, respectively and the value of $V^{R1}_{\max}$ was calculated as 169.5 mM/min by adopting the steady state concentrations of *Glc* and *ATP* (0.098 and 2.5 mM, respectively) from Teusink et al. [17] for the glucose rich condition (50 mM external steady state glucose) to fitting the glycolytic flux equal to that of the Teusink et al. model. Another rate equation for V^{R1} (HK-PFK) has been proposed by Heinrich and Schuster [18]. Comparison of the simulation results for both equations for dominoes of Figs. 1A, 3A and 4A in this manuscript is shown in Figs. S8, S9 and S10, respectively in the supplementary material.

2.1.1.2. Lower glycolysis domino. The second domino consumed *FbP* and four *ADP* molecules and produced two pyruvate and four ATPs. For the reasons of conciseness this domino was integrated with a third process converting pyruvate to ethanol and carbon dioxide (Fig. 1A). The reactions and rate expressions are shown below

$$FbP + 4ADP \rightarrow 2Pyruvate + 4ATP \quad (5)$$

$$\nu^{R2} = V^{R2}_{\max} \cdot \left(\frac{(FbP \cdot ADP)}{K_{mR2FbP} \cdot K_{mR2ADP} \cdot \left(1 + \frac{FbP}{K_{mR2FbP}} + \frac{ADP}{K_{mR2ADP}}\right)} \right) \quad (6)$$

$$Pyruvate \rightarrow Ethanol + CO_2 \quad (7)$$

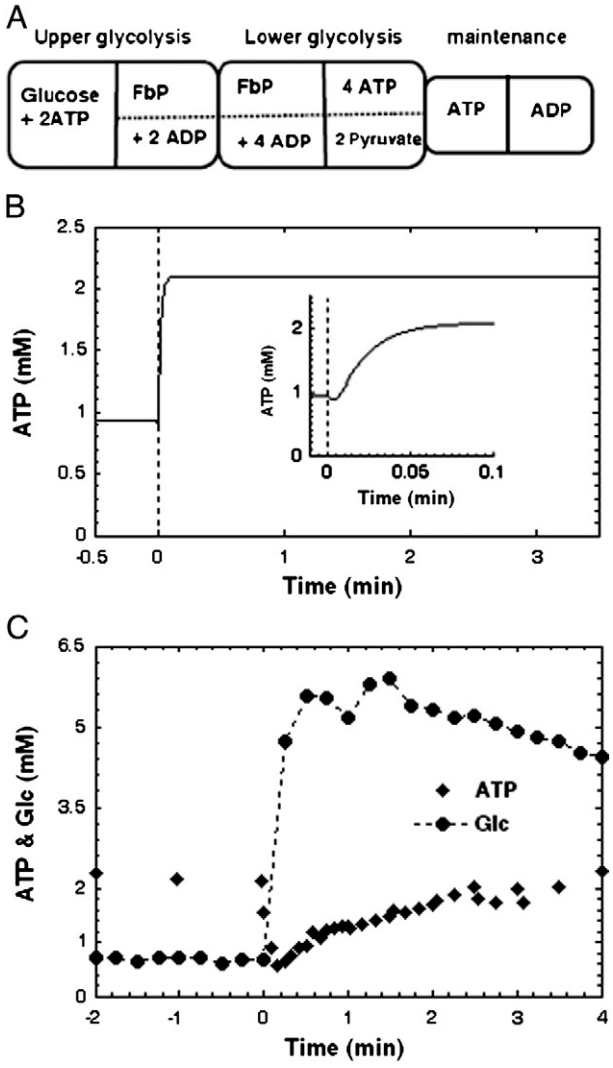

Fig. 1. (A): The domino of glycolysis split into two consecutive dominoes, i.e., upper glycolysis leading from glucose to fructose-1,6-bisphosphate (FbP) and lower glycolysis from FbP to pyruvate and 4ATPs and then further from pyruvate to ethanol and carbon dioxide (see Materials and methods). Glycolysis leads to the net production of two ATPs. On the right: the maintenance domino that persists. (B): Model calculations of ATP dynamics based on second domino scheme under glucose limited and excess conditions. Vertical dotted line indicates separation of glucose limited and rich conditions. (C): 'ATP paradox' observed in *S. cerevisiae* growing in glucose limited continuous anaerobic culture ($D = 0.1\ h^{-1}$ with steady state $C_{glc} = 0.67$ mM). After sudden addition of extra glucose (i.e. glucose increase to $C_{glc} = 5.56$ mM) at $t = 0$ the intracellular concentration of ATP rapidly and significantly decreases and recovers in 4 min, and only partly.

$$v^{R3} = V^{R3}_{\max} \cdot \left(\frac{PYR}{K_{mR3PYR} + PYR} \right). \tag{8}$$

Parameter values K_{mR2FBP}, K_{mR2ADP} and K_{mR2PYR} were taken as 0.3, 0.53 and 4.3 mM, respectively and the value of $V^{R2}_{\max}$ and $V^{R3}_{\max}$ were calculated equal to 186.2 and 266.8 mM/min by adopting the steady state concentrations of *FBP*, *ADP* and *PYR* from Teusink et al. [17] for the glucose rich condition (50 mM external steady state glucose) to make the glycolytic flux equal to that of the Teusink et al. model.

2.1.1.3. Combined glycolysis domino. Where indicated (Figs. 5–8) we also used a 'complete glycolysis domino', based on the Teusink model of glycolysis [17], with an explicit representation of ATP, ADP and AMP. We have replaced the fixed fluxes for trehalose and glycogen reactions in the Teusink model by fluxes given by rate equations in terms of irreversible mass action kinetics. The rate constants $k_{TREHALOSE}$ and $k_{GYCOGEN}$ were calculated as 0.9 and 2.31 $\text{min}^{-1}.(\text{mM})^{-1}$ to match the previously fixed flux values through these reactions while keeping metabolite (G6P and ATP) concentrations equal to the corresponding original steady state concentrations for the glucose rich condition (50 mM extracellular glucose). The flux for the ATPase reaction was split into two domino fluxes, one for maintenance and another for growth (see below).

2.1.2. Maintenance domino

This process consumes ATP energy to keep cellular machinery in the working state. Consumption of *ATP* for maintenance needs ~1 mmol/gDry-cell/h of *ATP* in carbon starvation condition [19]. Therefore this domino depends only on the *ATP* and consuming *ATP* as its turnover to *ADP* and P_i:

$$ATP \rightarrow ADP + P_i \tag{9}$$

$$v^{Maintenance} = k_{maintenance} \cdot [ATP]. \tag{10}$$

This led to an 8.3 mM/min maintenance flux, which was calculated by multiplying the 1 mmol/gDry cellweight/h *ATP* demand of *Saccharomyces cerevisiae* under carbon starving conditions [19] by 60 min/h and dividing it by 445 gDCW/Lcytosolic volume (Maksim Zakhartsev's unpublished data). Using an *ATP* concentration of 2.5 mM (the ATP concentration for the glucose rich condition in the Teusink et al. model), the parameter value $k_{maintenance}$ was calculated as 3.33 min^{-1} to meet the ~1 mmol/gDCW/h ATP demand of *S. cerevisiae*.

2.1.3. Growth domino (version 1)

The version-1 of growth is a minimal model of one reaction which consumes ATP and the glycolytic metabolite pyruvate as precursors of the biomass building blocks. The need of ATP for incorporation of one gram-atom carbon in biomass was calculated as 2–2.5 mol of ATPs using experimental data of biomass yield per mole of ATP and the $CH_{1.64}O_{0.52}N_{0.16}P_{0.01}S_{0.005}$ formula for biomass [20,21]. Later the stoichiometry of pyruvate and ATP for biomass synthesis was calculated as 1:6 for three C-atoms per mole of pyruvate. This reaction is modeled using irreversible Michaelis–Menten kinetics dependent on pyruvate and ATP.

$$Pyruvate + 6ATP \rightarrow Biomass + 6ADP \tag{11}$$

$$v^{Growth} = V^{Growth}_{\max} \cdot \left(\frac{Pyruvate \cdot ATP}{K_{mGrowth_{Pyruvate}} \cdot K_{mGrowth_{ATP}} \cdot \left(1 + \frac{Pyruvate}{K_{mGrowth_{Pyruvate}}} + \frac{ATP}{K_{mGrowth_{ATP}}} \right)} \right). \tag{12}$$

This equation is used for growth dominoes in Figs. 3A and 4A. The parameter values $K_{mGrowthPyruvate}$, $K_{mGrowthATP}$ were taken equal to 2.0 and 4.0 mM respectively, assuming that most of the reactions in a metabolic pathway operate at Michaelis–Menten constants close to intracellular concentrations at steady state. $V^{Growth}_{\max}$ was determined equal to 59.3 mM/min by fitting the data of ~10–15% of carbon (glucose) flux accumulates as biomass for yeast cells growing in anaerobic conditions [22,23].

2.1.4. Growth domino (version 2)

In a subsequent domino approach to growth, biomass synthesis was assumed to be allosterically regulated by the fructose-1,6-bisphosphate (*FbP*) concentration, which would act as a second monitor (in addition to pyruvate) of the carbon state of the cell:

$$v^{Growth} = V^{Growth}_{\max} \cdot \left(\frac{Pyruvate \cdot ATP}{K_{Growth_{Pyruvate}} \cdot K_{mGrowth_{ATP}} \cdot \left(1 + \frac{Pyruvate}{K_{mGrowth_{Pyruvate}}} + \frac{ATP}{K_{mGrowth_{ATP}}} \right)} \right) \times \left(\frac{FbP}{K_{sFbPGrowth} + FbP} \right). \tag{13}$$

Version 2 of the growth domino was used for Figs. 5–8. Parameter values $K_{mGrowthPyruvate}$, $K_{mGrowthATP}$ were kept as mentioned in growth domino (version 1) and $K_{sFbPGrowth}$ was taken as 0.12 mM, which is equal to the steady state concentration of *FbP* at a glycolytic flux half of the maximum flux in Teusink et al. [17]. V_{max}^{Growth} was calculated as 37.8 mM/min by fitting it to the observation that the data of ~10–15% (we assumed 12.5%) of carbon (glucose) flux accumulating as biomass for yeast cells growing under anaerobic conditions [22,23]. Glucose flux to trehalose and glycogen was also considered as carbon flux for growth.

2.1.5. Adenylate kinase domino

Adenylate kinase provides a link between the substrate energy molecule *ADP* and the product energy molecule *ATP* of glycolysis through *AMP*. It transphosphorylates two *ADP* molecules to an *ATP* and *AMP* molecule:

$$2ADP \Leftrightarrow ATP + AMP \tag{14}$$

$$v^{AK} = k_{Ak} \cdot \left(ADP^2 - \frac{ATP \cdot AMP}{K_{eqAK}} \right). \tag{15}$$

Parameter values k_{AK} and K_{eqAK} were taken equal to 1330.33 mM/min and 0.45 as reported in [17].

2.1.6. AXP consumption for biomass domino

DNA and RNA together constitute ~20% (dry w/w) of biomass of *S. cerevisiae* growing in anaerobic condition [22]. Accordingly, the AXP consumption for biomass domino was modeled to incorporate ATP for nucleotides in DNA and RNA as ~20% (w/w) of biomass. So ATP flux to biomass was calculated by considering mass ratio of average molecular weight of nucleotides (330 Da) in DNA/RNA and glucose, which calculates net 14% of growth flux (pyruvate incorporation flux in biomass). Glucose flux to trehalose and glycogen was also considered as carbon flux for growth. This domino was kept coupled with growth domino.

$$ATP \rightarrow Biomass \tag{16}$$

$$v^{ATP_Biomass} = 0.14 \cdot V^{Growth} \tag{17}$$

2.1.7. Nucleotide biosynthesis domino

Because cell growth will gradually deplete the nucleotide pool, a domino that replenishes the pool was introduced. The glycolytic precursor for AMP synthesis via the pentose phosphate pathway is G6P and turn-over of five ATP molecules in various steps in the salvage pathway [24]. The flux for this reaction was taken corresponding to ~20% of the carbon flux for biomass synthesis as described in 'AXP consumption for biomass domino':

$$G6P + 5 \cdot ATP \rightarrow AMP + 5 \cdot ADP \tag{18}$$

$$v^{nucleotide_synthesis} = 0.14 \cdot V^{Growth}. \tag{19}$$

2.1.8. Adenine nucleotide salvage domino

In the presence of *ATP*, *AMP* was preferentially degraded via *IMP* and appeared in the form of inosine and hypoxanthine [25]. This domino assumes that at lower concentrations of *ATP*, *AMP* deaminates to *IMP* and further dephosphorylates to inosine. Also, *AMP* dephosphorylates to adenosine;

$$AMP \Leftrightarrow IMP \tag{20}$$

$$v^{AMPdeaminase} = k_{AMPdeaminase} \cdot \left(AMP - \frac{IMP}{K_{eqAMPdeaminase}} \right) \tag{21}$$

$$IMP \Leftrightarrow Inosine \tag{22}$$

$$v^{IMPPhosphatase} = k_{IMPPhosphatase} \cdot \left(AMP - \frac{IMP}{K_{eqIMPPhosphatase}} \right) \tag{23}$$

$$AMP \Leftrightarrow adenosine \tag{24}$$

$$v^{AMPnucleotidase} = k_{AMPnucleotidase} \cdot \left(AMP - \frac{IMP}{K_{eqAMPnucleotidase}} \right). \tag{25}$$

These reactions are catalyzed by different enzymes in the forward and reverse directions [25] but metabolite data produced in this study indicate that they quickly reach to equilibrium. So, our model assumed that the above reactions are very fast like the adenylate kinase reaction in Teusink model [17]. The *k* values for these reactions were taken equal to k_{AK} for adenylate kinase reaction of value 1330.33 mM/min. All three K_{eq} were estimated equal to ~0.7 by taking the ratios corresponding to metabolites in the glucose limited chemostat cultures. Under the transient condition after the glucose pulse, the above reactions were not at equilibrium. The various 'dominoes' in the model were developed using MATLAB (The Math Works Inc., U.S.A.) and COPASI software and parameter values used in the model are given in Supplementary material Table S1.

2.2. Experimental procedures

2.2.1. Strains, medium and cultivation conditions

S. cerevisiae CEN.PK 113-7D were grown anaerobically in glucose limited chemostat on anaerobic minimal synthetic CEN.PK medium prepared according to [26]. The chemostat (steel KLF 2.5 L bioreactor; Bioengineering, Switzerland) operating conditions were: $D = 0.1\ h^{-1}$, feeding $C_{glc} = 278$ mM, T = 30 °C, pH = 5.0 (adjusted by KOH), $pO_2 =$ 0% (constant nitrogen sparging through the culture with 1.5 L min^{-1}), $P_{headspace} = 0.3$ bar, stirring at 400 rpm. Under these operating conditions the yeast culture reaches the following steady state properties: cell density $C_x = 3.5$ gDW/L and glucose concentration $C_{glc} = 0.67$ mM.

2.2.2. Glucose perturbation and sampling

After the yeast culture had reached the steady state it was perturbed with a glucose increase: At $t = 0$ min the extra glucose ($C_{glc} = 5.56$ mM) was injected directly into the chemostat. Samples were withdrawn from the chemostat both during steady state phase and during 30 min after glucose perturbation with different time intervals. Rapid sampling was performed by a computer aided sampling robot that withdraws the required amount of the broth (1.5 mL) at designed time points with 1 mL/s into 9 mL of pure −50 °C methanol.

2.2.3. Sample preparation and analytical methods

Upon sample collection they were immediately centrifuged at 20,000×*g* for 3 min at −20 °C, and the cell pellets were separated from the supernatants. Prior to the extraction, the cold pellet was heat shocked at +90 °C for 15 s, and only then immediately extracted with 3 mL of hot pure ethanol +90 °C during 5 min with vortexing once per minute. Then the extracts were immediately cooled down on ice/water bath at 0 °C and further evaporated in rotational vacuum concentrator (Christ® RVC 2–33 IR, 4 mbar, ~1 h under 4 °C) to dryness. The remains were re-dissolved in 1000 μL of 10 mM phosphate buffer pH 7.0, vortexed well and then 500 μL of chloroform was added, vortexed well and centrifuged 5 min at

20×10^3 *g* at 4 °C. Then 200 μL of aquatic phase was collected and used for HPLC analysis. Agilent 1200 Series HPLC system was used with Supelcosil™ LC-18-T column (3 μm; 150×4.6 mm; Supelco, USA) guarded with Supelcosil™ LC-18-T Supelguard™ (3 μm; 20×4.0 mm; Supelco, USA). Buffer A: 100 mM phosphate buffer pH 6.0; 4 mM tetrabutylammonium disulfate (TBAS). Buffer B: 30% methanol in 100 mM phosphate buffer pH 7.2 and 4 mM TBAS. The separation was performed in linear gradient from 0 to 100% of B with 1.5% min^{-1} and flow rate 1 mL min^{-1} at 25 °C (column thermostat) and detection at 260 and 340 nm. The separation method was calibrated using ATP, ADP and AMP (Sigma) as standards and further the AXP content was expressed in μmol per gram of dry weight of biomass [μmol/gDW].

3. Results

3.1. The first domino: connecting glycolysis to ATP

The composition of the biomass in terms of elements (C, N, P, and S), electrons (H/O) and Gibbs free energy is virtually constant. Consequently under any given growth condition usually all but one, are present in excess. Here we shall develop the case where the Gibbs free energy limits growth. The most important commodities for Gibbs free energy in Biology are the hydrolytic free energy of ATP and the trans-membrane electrochemical potential for protons across the inner mitochondrial (eukaryotes) or plasma (prokaryotes and Archaea) membrane. For simplicity we here choose an experimental system where the former is definitely the more important of the two. This defines the value of one side of the first domino.

The domino itself should then be a process that synthesizes ATP from a different commodity. Because we here wish to illustrate the domino approach we choose a relatively simple but fully relevant experimental system, i.e. ATP synthesis powered by the breakdown of glucose to alcohol and carbon dioxide in baker's yeast: The first domino (Supplementary material Fig. S1) is glycolysis that starts from glucose and leads to ATP. The chemical reaction corresponding to this first domino is:

$$glucose + 2ADP + 2P_i \rightarrow 2ethanol + 2CO_2 + 2ATP.$$

This reaction has a highly negative standard Gibbs energy, so that by itself it will phosphorylate virtually all ADP to ATP under ambient conditions if it is allowed to proceed to equilibrium. The second column in Table 1 shows the concentrations of ATP and ADP obtained in a glucose limited chemostat culture of baker's yeast. The ATP concentration exceeds the concentration of ADP but the latter is not close to zero. The first domino is not enough to explain this experimental result of a limit to the phosphorylation of ADP. This conclusion is independent of any parameter value other than Gibbs free energies of ATP hydrolysis and glucose fermentation, which are well known.

3.2. The second domino: maintenance

Living organisms are not at thermodynamic equilibrium. They consume ATP in biosynthetic reactions as well as for physiological maintenance [27]. The latter process corresponds to the maintenance domino that leads from ATP to ADP (Supplementary Fig. S1, right-hand side). The fourth column in Table 1 shows the result of calculations of the steady state for a realistic model of glycolysis [17], plus an estimated module summarizing the maintenance processes. With this maintenance module the ADP modeled for excess glucose exceeded zero and can be fitted to the experimental value.

Table 1
In vivo and in silico adenine nucleotide concentrations in *S. cerevisiae* growing under glucose limited and excess conditions, as determined experimentally and calculated by the model.

Metabolites	Chemostat experiment		Teusink model	
	Glucose limited (5 min before)	Glucose excess (10 min after)	Glucose limited (5 min before)	Glucose excess (10 min after)
ATP (mM)	2.2	1.9	1.34	2.3
ADP (mM)	1.1	0.9	1.7	1.4

3.3. The ATP paradox and the dynamics of glycolysis

Because the experiment was carried out in a glucose limited chemostat at a dilution rate (and hence at a specific growth rate) of 0.1 h^{-1}, far below the maximum growth rate, the glucose concentration could not have been saturating growth. Hence, the model with glycolysis and maintenance simulated an increase in the ATP level upon addition of excess glucose (Table 1, columns 4 and 5). This prediction was however not in keeping with our experimental results: here ATP was constant or perhaps subject to a slight decrease (see Table 1, columns 2 and 3). The prediction is not in line either with the earlier observation by Theobald et al. [28] that upon glucose addition to a glucose limited chemostat, ATP decreased significantly. The failure of ATP to increase upon addition of glucose is what we call the glucose-ATP paradox.

Like most catabolic pathways, glycolysis is activated by the coupling of early reactions to the dephosphorylation of ATP, in thereby thermodynamically downhill reactions. Further down the pathway four ADP molecules are phosphorylated to ATP leading to a net yield of two ATPs. Perhaps therefore, the decrease in ATP observed by Theobald et al. [29], was due to this first phase dominating the dynamics. Under our precise experimental conditions the two effects of an early decrease and a subsequent increase might be confounding the earlier prediction.

This complication suggests that we should split up the glycolysis domino into two consecutive ones, i.e. one leading to the synthesis of fructose bisphosphate at the expense of two ATPs and one leading from fructose bisphosphate to alcohol, carbon dioxide and 4ATPs. Fig. 1A shows the resulting domino scheme and Fig. 1B the corresponding calculations of ATP dynamics, where true fluxes and intracellular concentrations are taken into account. Indeed, the calculations show that initially the ATP level slightly decreases after glucose addition (Fig. 1B inset), which is followed by a dominant increase that leads to an ATP level that is higher than the initial level. A sensitivity analysis indicated that qualitatively this observation did not depend on any parameter value in the model (see supplementary material). Clearly, the issue cannot be resolved in an experiment taking a single time measurement (as in Table 1), but requires a time series experiment. Fig. 1C shows the results of such an experiment at high time resolution. The experiment reveals that indeed there is a sharp drop in ATP levels upon addition of the glucose, which is followed by an almost equally acute increase. Splitting the glycolysis module into two components not only explains the transient drop in ATP, but also demonstrates that for the comparison of the steady states before and after addition of extra glucose, the existing domino model (Fig. 1A) is insufficient.

3.4. The ATP paradox and growth rate acceleration

Under the conditions of the experiment of Table 1 and Fig. 1C, the cells are growing under glucose limiting conditions (in a chemostat). Consequently, one should expect that the addition of excess glucose should increase the rate at which the cells grow. We therefore added the domino of growth itself, as energized by ATP. Fig. 2 shows the corresponding domino scheme and calculations of ATP dynamics. Also this new model predicts that upon addition of excess glucose the steady-state ATP level should increase (Fig. 2B) after increasing the extracellular glucose concentration. This observation

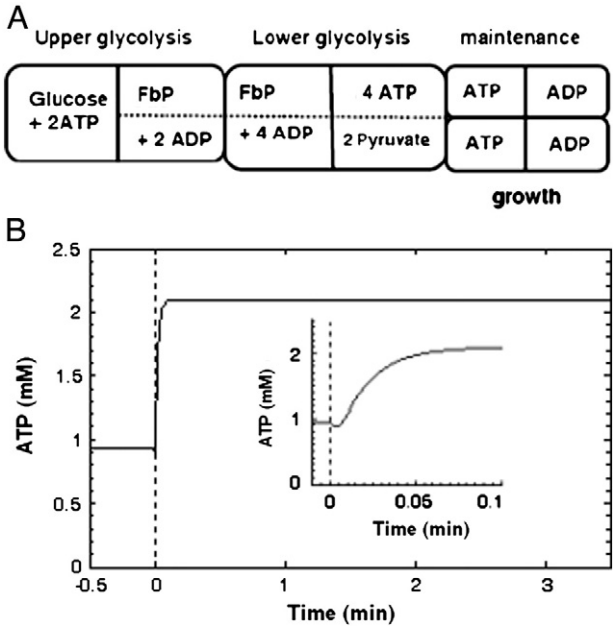

Fig. 2. (A): Schematic of glycolysis split in two dominoes; Upper glycolysis leading from glucose to fructose-1,6-bisphosphate (FbP) and lower glycolysis from FbP to pyruvate and net production of two ATP and further pyruvate is converted to ethanol and carbon dioxide. Consumption of ATP is split into the two dominoes, maintenance and growth. (B): Simulation of ATP dynamics based on scheme 2A under glucose limited and rich conditions. Vertical dotted line indicates separation of glucose limited and rich conditions.

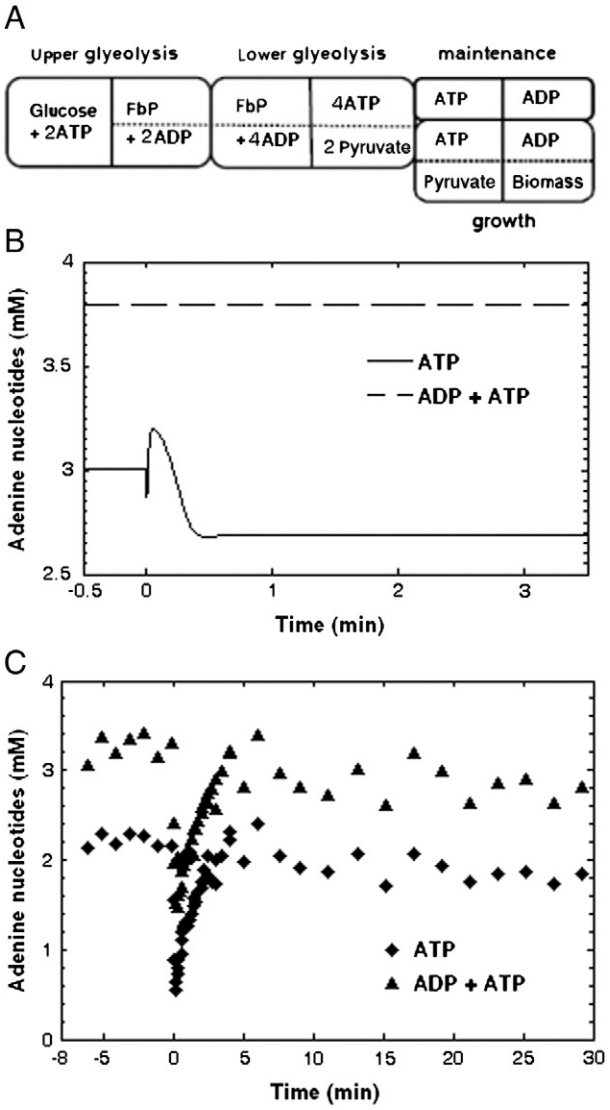

Fig. 3. (A): Domino scheme of (i) upper glycolysis leading from glucose to fructose-1,6-bisphosphate (FbP) and (ii) lower glycolysis from FbP to ATP and pyruvate and pyruvate to ethanol and carbon dioxide, (iii) maintenance hydrolyzing ATP, and (iv) growth now depending on both ATP and pyruvate. (B): Model calculations of the adenine nucleotides corresponding with the domino scheme of panel A under conditions of glucose-limited followed (at $t=0$) by glucose-excess conditions. (C). The 'ATP + ADP puzzle' observed in yeast growing in glucose limited continuous culture and supplemented with excess glucose as shown in Fig. 1C.

did not depend on values on the parameters in the model (see supplementary material). This is understandable as in this model growth rate can only increase if the ATP level increases. The two dominoes for maintenance and growth appear to be functionally identical in Fig. 2A. Nevertheless these model predictions are in flagrant contrast to experimental observations (Fig. 1C).

Growth does not only consume ATP but also carbon, and the domino scheme of Fig. 2A neglects the latter. If both energy and carbon would be limiting growth at the same time, then Fig. 3A should be more appropriate, where we have now added a second intermediary between processes, i.e. a building block for the carbon content of biomass. Candidates for this are substances like pyruvate and glucose-6-phosphate. Fig. 3B shows a calculation for when pyruvate is used as the second intermediate between glycolysis and growth. The calculation in Fig. 3B shows that now the ATP goes down slightly upon the addition of glucose, which is more in line with the experimental findings (Fig. 1C) and Theobald et al. [28].

In our calculations the growth rate was taken to depend rather strongly on the concentration of pyruvate. Our theoretical analyses suggested that whether the ultimate level of ATP would be lower or higher than the initial level for the transition from glucose limited to rich conditions (data not shown) should depend on the elasticities of growth for ATP relative to the elasticity of growth for the internal carbon source (intracellular glucose or glycolytic metabolite) stimulating growth [30]. With 'elasticity' we refer to the dependence of growth rate on the concentration of ATP or the carbon source. If growth depends more on ATP levels than on the internal carbon source, then upon stimulation of catabolism the increase in ATP would much stimulate growth and reduce the level of the carbon source, but if it depends more on the carbon source than on ATP, the carbon source would increase growth and pull down the ATP level. We conclude that the domino analysis now requires not only three processes but also two intermediates (ATP and carbon) to be considered.

3.5. The adenine nucleotide puzzle

In the standard views of cellular energetics, the terminal phosphate bond of ATP plays the central role; Gibbs energy extracted in catabolic processes is put into the phosphorylation of ADP to form ATP. The hydrolysis of this terminal phosphate anhydride bond is used to drive intracellular reactions that require Gibbs free energy. This is one of the 'bow-tie' schemes of cell function [27,31,32]. In this view the decreases in the concentration of ATP should be accompanied by equal increases in the concentration of ADP such that the sum concentration of ATP and ADP should remain unchanged. Fig. 3C shows that this was not quite the case experimentally: upon the addition of glucose there was a rapid decrease in the level of ATP, but the level of ADP did not increase by the same amount. The sum of the concentrations of ATP and ADP decreased rapidly and then increased again, slowly. Only after some 4 min the total level of ATP + ADP had returned to the original level.

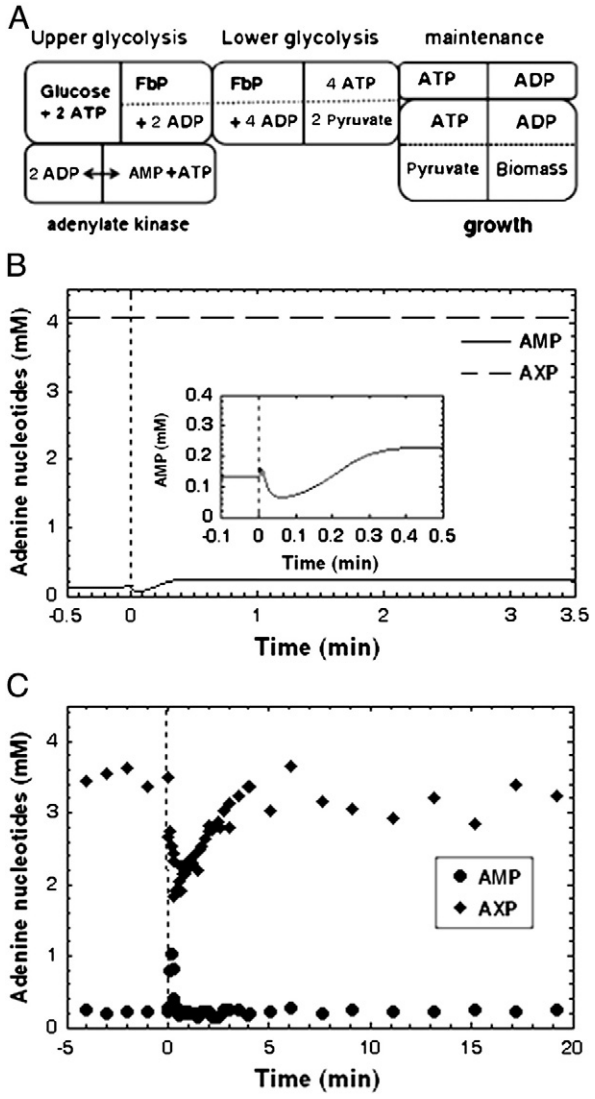

Fig. 4. (A): Domino systems biology scheme of glycolysis, maintenance and growth including adenylate kinase reaction, which equilibrates two molecules of ADP with AMP and ATP. (B): Model calculations of the adenine nucleotides corresponding with the schematic shown in panel A under glucose limited and excess conditions. (C): AMP and AXP dynamics observed in yeast growing in glucose limited continuous culture and supplemented with excess glucose conditions as shown in Fig. 1C. Vertical dotted line indicates separation of glucose limited and rich conditions. AXP refers the adenylate pool, where AXP = ATP + ADP + AMP.

One potential explanation for this phenomenon is the adenylate kinase reaction, in which 2 molecules of ADP transphosphorylate to produce one molecule of ATP and one molecule of AMP. The right-hand side of Fig. 4A has the corresponding domino, where it should be noted that it becomes hard to illustrate all implications by this two dimensional way of plotting. In particular the yield of ATP in this process is not well represented in the figure, but is taken into account in the calculations, the results of which are shown in Fig. 4B. Fig. 4B shows that indeed the sum of ATP and ADP should be expected to *decrease* upon the addition of glucose, because of a transient increase in the concentration of AMP. This then provided for a possible explanation of the transient decrease in the concentration of ATP + ADP.

In order to validate this explanation, we also measured the concentrations of AMP as a function of time (Fig. 4C). Although the concentration of AMP increased quickly and transiently upon addition of the excess glucose, the amplitude of the increase was much smaller than the extent of decrease in ATP + ADP. Clearly, although the addition of the new domino of adenylate kinase had some relevance, it did not suffice to explain the experimental observations. In Fig. 4B we also plot the sum of the concentrations of all adenine nucleotides. Up to this point the model has predicted this to be constant whereas in the experiments this sum concentration decreased strongly though transiently upon addition of glucose. This is what we call the 'adenine nucleotide puzzle'.

In the literature, bottom–up models are available for the dynamic behavior of glycolysis inclusive of maintenance and the adenylate kinase reaction. These are maximally based on experimental data of the component enzymes. Here we replace the more primitive models for the various dominoes for glycolysis, maintenance and adenylate kinase we used above, with a domino corresponding to the detailed model of Teusink et al. [17] (see Materials and methods). Fig. 5 shows that the conclusions achieved until now remain the same: all features can be explained except for the transient decrease in total adenine nucleotide concentrations that we observe experimentally upon the addition of excess glucose.

3.6. The adenine nucleotide puzzle and growth

The model arrived at up to this stage had a constant sum of concentrations of the adenine nucleotides. Growth implies the generation of new biomass. The new biomass will contain DNA, RNA, with dATP and ATP incorporated and indeed ATP, ADP and AMP as such, all of which would be made at the expense of the pool of ATP, ADP and AMP of the mother cell. We estimated the implications for a possible decrease of the sum adenine nucleotide concentrations in the dividing cells, assuming there were no re-synthesis. The results are shown in Fig. 6B. In this calculation we started from zero growth rate, enabling a steady state before the addition of the glucose which induced growth. The rate of decrease of the total adenine nucleotides pool that we calculated to be of the order of 1.3 mM/min is not in line with the kinetics observed experimentally in Fig. 4C. The AXP drop in the calculation has a half life time of ~1.5 min,

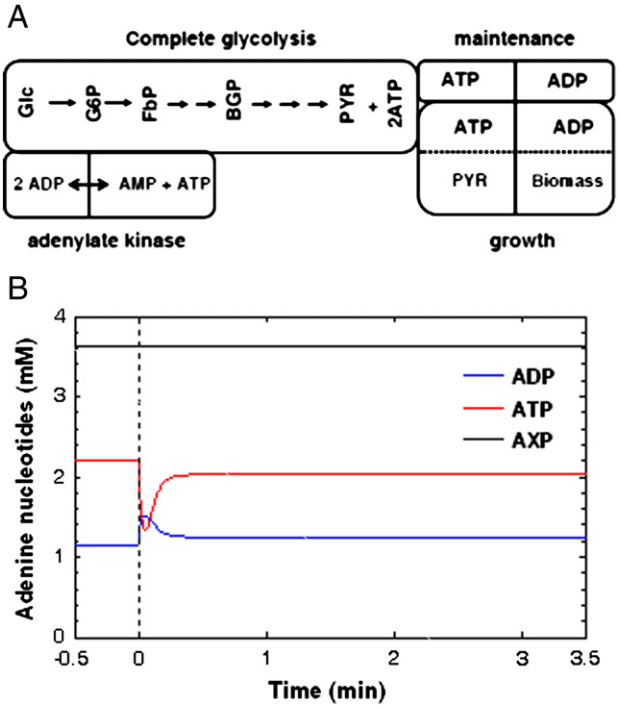

Fig. 5. (A): Schematic of complete glycolysis model [17] with equilibration by adenylate kinase, maintenance and growth dominoes. Maintenance consumes ATP for the maintenance of old biomass and growth consumes pyruvate and ATP for the synthesis of new biomass. (B): Model simulated profiles of adenine nucleotides for the integrated dominoes shown in panel A.

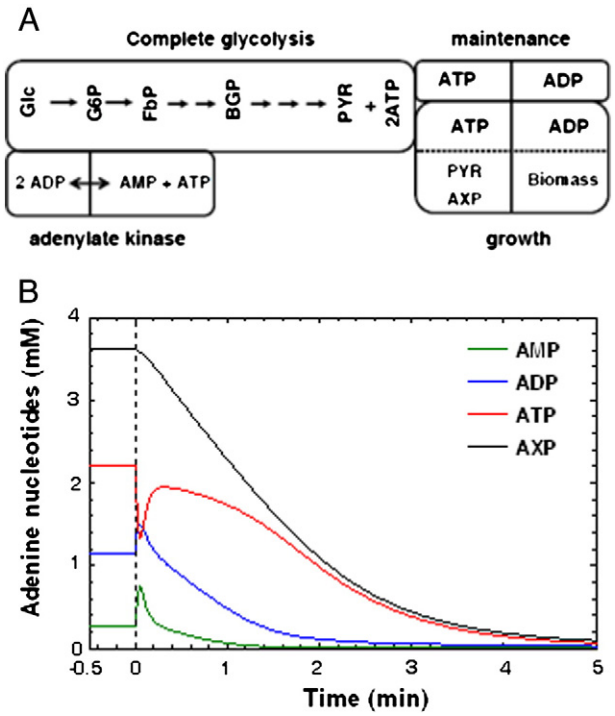

Fig. 6. (A). Schematic of a more complete domino model incorporating AXP into biomass. Complete glycolysis with adenylate kinase, which equilibrates the reaction of two molecules of ADP to AMP and ATP. Maintenance module consumes ATP to maintain the old biomass. Growth module consumes ATP, carbon as pyruvate for synthesis of new biomass and also incorporates AXP in the new biomass. (B) Calculated decrease in adenine nucleotides using a growth domino that incorporates adenine nucleotides into new biomass (A). This domino model includes modules of glycolysis, maintenance and growth as carbon status of cell, ATP turn-over and ATP incorporation as ~20% of carbon flux for biomass for the synthesis of DNA and RNA for new biomass. Vertical dotted line indicates separation of glucose limited and excess conditions.

whereas the drop in the experiments has a half time that is more than 10 times faster. Also, this model predicts a persistent drop in AXP level at a half life of some 4 min, which is at odds with the experimental finding of a return of AXP levels to normal within 5 min of the glucose perturbation (Fig. 4B).

Of course, when adenine nucleotides are being consumed in biomass synthesis they should also be re-synthesized. Otherwise there will eventually be a shortage that will shut down all processes for lack of ATP. We examined a number of options for inserting this new domino into the domino model (Fig. 7A). We first introduced an AMP re-synthesis process at a constant rate just enough to compensate for the adenine nucleotide consumption at the low growth rate before the addition of extra glucose. This had the effect that after glucose addition, adenine nucleotides would still run out within 5 min. This problem persisted in models where AMP re-synthesis was inhibited by ATP [24], stimulated by AMP, which led to a catastrophic depletion of adenine nucleotides ultimately, and inhibited by AMP.

We then asked whether there was a regulatory design where the sum of the adenine nucleotides would not be affected by their increased consumption due to the addition of glucose. We observed that an effective way of doing this would be to make the rate of re-synthesis of AMP a direct function of the carbon status of the cell, in the same sense as growth rate itself. The corresponding calculations (Fig. 7B and C) show that this would work partly: Here the sum of the adenine nucleotides would not decrease in a sustained manner. However, this domino did not reproduce the transient but strong decrease in sum adenine nucleotides during the first 5 min after glucose addition.

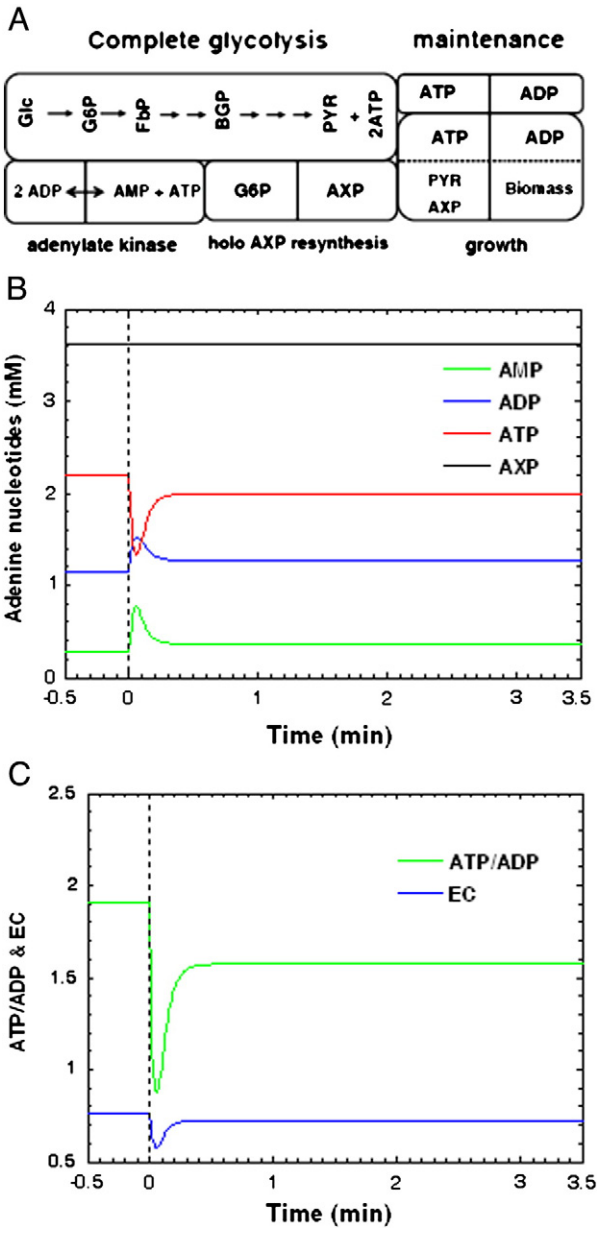

Fig. 7. (A). Domino model with AXP resynthesis. The growth domino consumes ATP, carbon as pyruvate for synthesis of new biomass and also incorporates AXP in the new biomass. The holo AXP resynthesis module synthesizes AMP from G6P to compensate the AXP incorporated in the biomass. (B). Dynamics of the individual nucleotides (ATP, ADP, AMP and AXP). (C). Dynamics of the ATP/ADP and the Energy Charge (EC). Growth was taken dependent on pyruvate and ATP, and regulated by fructose-1,6-bisphosphate concentration. Incorporation of AXP in biomass was taken as dependent on ATP coupled with growth domino. The AMP synthesis domino was added to compensate for the AXP depletion due to growth and was taken as dependent on glucose-6-phosphate and ATP and coupled with growth domino. Vertical dotted line indicates separation of glucose limited and excess conditions.

3.7. The adenine nucleotide puzzle: IMP salvage domino

The rapid depletion of the total adenine nucleotide pool that sets in motion upon glucose addition could also be driven by a process decomposing AMP and regulated by the concentration of AMP. Therefore we next considered the domino corresponding to this. IMP is the deaminated product of AMP in the adenine degradation salvage pathway, and a metabolite in biosynthetic and salvage pathways of purine nucleotides [24]. Indeed (Fig. 8B) we observed a transient accumulation of IMP. We therefore added two dominoes, i.e. one for the decomposition of AMP into IMP, driven by the concentration of AMP,

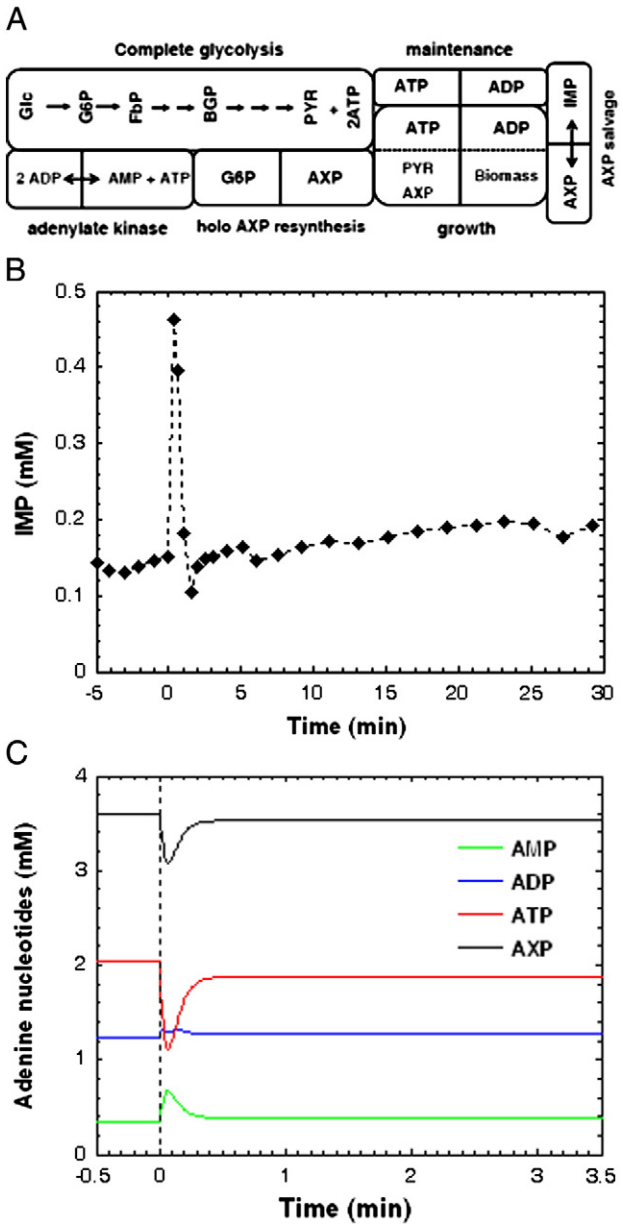

Fig. 8. (A). The domino model including the nucleotide salvage pathway. The new module AXP salvage includes metabolism of AMP to its deaminated metabolites and resynthesis. (B) Experimentally observed dynamics of inosine monophosphate (IMP) in yeast growing on glucose limited continuous culture and supplemented with excess glucose conditions as shown in Fig. 1C. (C) Dynamic of individual adenine nucleotides for transition from glucose limited to excess conditions for the ultimate domino model that includes AXP salvage. The adenine nucleotide metabolism module is added which includes adenylate kinase type equilibration reactions of AMP to adenosine, AMP to IMP and IMP to inosine, as detailed under Materials and methods. Vertical dotted line indicates separation of glucose limited and excess conditions.

and one for the resynthesis of AXP from IMP. In Fig. 8A these are shown as a single domino called AXP salvage.

The calculated dynamics of adenine nucleotide energy charge are shown in Fig. 8C. This domino model can explain experimental observations shown in Figs. 3C and 4C for the dynamics of ATP, ADP, AMP and AXP all together, as well as the dynamics for IMP.

4. Discussion

The complexity of living cells hampers the understanding of biological functioning. Simplifying approaches are not without risk [33], but comprehensive approaches such as bottom–up and top–down systems biology require too much mechanistic information or too many experimental perturbations. Therefore we here developed a new systems biology approach and showed that it generated discoveries and understanding in energy and carbon metabolism in yeast. Truly new aspects of the domino approach are the fact that there are modules that each has a limited number of explicit inputs and a limited number of explicit outputs. Consequently, the various modules can be integrated readily into domino pathways. These pathways enable one to follow flows of interaction and information through the system, from one input to various outputs for instance. This domino approach should be very suited for integrating the understanding contributed by various research groups into a process that leads to understanding a whole biological system in terms of the functioning of and interactions between its functional components. The building of integral models in terms of component models is becoming important for metabolic engineering and truly individualized therapy of human disease [34].

The salvage pathway of adenine nucleotides was known biochemically, and so were the glycolytic pathway, the phenomenon of maintenance, and the fact that the synthesis of new biomass can go at the cost of the sum of ATP, ADP and AMP. However, these and other phenomena highlighted above have not yet been brought to bear on the single issue of growth and its dependence on the level of glucose, the molecule delivering the required free energy and carbon. This single perspective has enabled us to assess the quantitative importance of the incorporation of adenine nucleotides into new biomass, and the importance of the dependence of growth rate on both carbon and ATP levels. And then, where in the usual bow-tie models [27,31], the ATP–ADP ratio would be the prime and perhaps sole intermediate between catabolism and anabolism, we here find that the center of the bow-tie is more complex and also comprises the sum adenine nucleotide concentration, which is sustained by the adenine nucleotide salvage pathway.

Uwe Theobald was first to observe the 'ATP paradox', in *S. cerevisiae* growing in aerobic chemostat [29]. More thorough analysis of dynamic metabolite concentrations in the course of the glucose perturbation [28], allowed the testing of more extended yeast dynamic models [35], which however did not match the experimental observations of the AXP dynamics either. In order to improve data quality, sophisticated rapid sampling devices have been designed [for review [36]], as well as better techniques for quenching [for example [37]] and sample preparation [for example [38,39]]. Various analytical quantification techniques [for example [38,40]] were developed to collect unbiased metabolite dynamics even on sub-second time scales [for example [41]]. All these more refined studies confirmed the ATP paradox in yeast both under aerobic and anaerobic conditions. There were several hypotheses to explain the dynamic decrease of ATP concentration in the course of the glucose perturbation in yeast:

1. use of ATP for glucose phosphorylation by glycolysis [17,28,35]
2. use of ATP for anabolic processes [30,35]
3. consumption of ATP for polymerization reactions, i.e. RNA synthesis (this paper).

Our domino approach was able to assess the relative importance of these mechanisms. Will this make a difference? For those who doubt that it will, it may be worth noting that current models of yeast metabolism assume that the adenylate pool constitutes a *conserved moiety* [17,35], which is not the case at time scales faster than 4 min (Fig. 1C). Not only the ATP concentration, but also the AXP changes over the transition from a glucose limited to a glucose excess scenario. In this regard the third hypothesis looked most attractive to explain the dynamics of AXP. However, contrary to earlier assumptions, we here showed that the observed drop in ATP could neither be entirely attributed to the hydrolysis of ATP for energy transfer process such as glucose phosphorylation [28], nor to the

increase in RNA synthesis [42]: The glucose increase induces a fast activation of the purine salvage pathway as indicated by the transient drop of ATP and ADP with concomitant rise of IMP and inosine, both in our experimental data and in those of Loret et al. [43]. Counterbalancing the loss of AXP, the purine biosynthesis and salvage pathways are upregulated in a concerted manner, reflecting a sudden increase of the purine demand [42]. In this paper we have put this all in a complete and domino-ed perspective and have shown that now the glucose limited chemostat growth of yeast and the subsequent addition of glucose can be understood in terms of a single model.

The domino systems biology peruses the systems biology spiral of the model development: the iteration model ⇆ experiment turning into a spiral into the third dimension of understanding, where each round of the model development is compared with current experimental result or generates the need for the further experiments. Further turns of the spiral should pinpoint the involvement of the internal carbon signal (pyruvate and fructose bisphosphate were initial proposals), and the redox dimension.

Acknowledgement

The authors thank the transnational Systems Biology of MicroOrganisms (SysMO) program and its funders for the support of the MOSES project and all the partners of MOSES consortium for discussion. HVW also thanks other contributing funding sources such as EPSRC/BBSRC (BB/F003528/1, BB/C008219/1, BB/F003544/1, BB/I004696/1, BB/I00470X/1, BB/I017186/1, EP/D508053/1, BB/I017186/1), NWO, and EU-FP7 (EC-MOAN, UNI-CELLSYS).

Appendix A. Supplementary data

Supplementary data to this article can be found online at http://dx.doi.org/10.1016/j.bbabio.2012.09.014.

References

[1] S. Brenner, D. Noble, T. Sejnowski, R.D. Fields, S. Laughlin, M. Berridge, L. Segel, K. Prank, R.E. Dolmetsch, Understanding complex systems: top–down, bottom–up or middle-out? in: G. Bock, J. Goode (Eds.), Novartis Foundation Symposium: Complexity in Biological Information, John Wiley, Chichester, 2001, pp. 150–159.
[2] P. Kohl, D. Noble, Systems biology and the virtual physiological human, Mol. Syst. Biol. 5 (2009).
[3] A. Wagner, The yeast protein interaction network evolves rapidly and contains few redundant duplicate genes, Mol. Biol. Evol. 18 (2001) 1283–1292.
[4] K.R. Christie, S. Weng, R. Balakrishnan, M.C. Costanzo, K. Dolinski, S.S. Dwight, S.R. Engel, B. Feierbach, D.G. Fisk, J.E. Hirschman, E.L. Hong, L. Issel-Tarver, R. Nash, A. Sethuraman, B. Starr, C.L. Theesfeld, R. Andrada, G. Binkley, Q. Dong, C. Lane, M. Schroeder, D. Botstein, J.M. Cherry, Saccharomyces genome database (SGD) provides tools to identify and analyze sequences from saccharomyces cerevisiae and related sequences from other organisms, Nucleic Acids Res. 32 (2004) D311–D314.
[5] A.H.Y. Tong, G. Lesage, G.D. Bader, H. Ding, H. Xu, X. Xin, J. Young, G.F. Berriz, R.L. Brost, M. Chang, Y. Chen, X. Cheng, G. Chua, H. Friesen, D.S. Goldberg, J. Haynes, C. Humphries, G. He, S. Hussein, L. Ke, N. Krogan, Z. Li, J.N. Levinson, H. Lu, P. Ménard, C. Munyana, A.B. Parsons, O. Ryan, R. Tonikian, T. Roberts, A.-M. Sdicu, J. Shapiro, B. Sheikh, B. Suter, S.L. Wong, L.V. Zhang, H. Zhu, C.G. Burd, S. Munro, C. Sander, J. Rine, J. Greenblatt, M. Peter, A. Bretscher, G. Bell, F.P. Roth, G.W. Brown, B. Andrews, H. Bussey, C. Boone, Global mapping of the yeast genetic interaction network, Science 303 (2004) 808–813.
[6] L. Magtanong, C.H. Ho, S.L. Barker, W. Jiao, A. Baryshnikova, S. Bahr, A.M. Smith, L.E. Heisler, J.S. Choy, E. Kuzmin, K. Andrusiak, A. Kobylianski, Z. Li, M. Costanzo, M.A. Basrai, G. Giaever, C. Nislow, B. Andrews, C. Boone, Dosage suppression genetic interaction networks enhance functional wiring diagrams of the cell, Nat. Biotechnol. 29 (2011) 505–511.
[7] R.O. Linden, V.P. Eronen, T. Aittokallio, Quantitative maps of genetic interactions in yeast—comparative evaluation and integrative analysis, BMC Syst. Biol. 5 (2011) 45.
[8] M. Schuldiner, S.R. Collins, N.J. Thompson, V. Denic, A. Bhamidipati, T. Punna, J. Ihmels, B. Andrews, C. Boone, J.F. Greenblatt, J.S. Weissman, N.J. Krogan, Exploration of the function and organization of the yeast early secretory pathway through an epistatic miniarray profile, Cell 123 (2005) 507–519.
[9] K. van Eunen, J. Bouwman, A. Lindenbergh, H.V. Westerhoff, B.M. Bakker, Time-dependent regulation analysis dissects shifts between metabolic and gene-expression regulation during nitrogen starvation in baker's yeast, FEBS J. 276 (2009) 5521–5536.
[10] H. Jeong, S.P. Mason, A.L. Barabasi, Z.N. Oltvai, Lethality and centrality in protein networks, Nature 411 (2001) 41–42.
[11] J. Rung, T. Schlitt, A. Brazma, K. Freivalds, J. Vilo, Building and analysing genome-wide gene disruption networks, Bioinformatics (Suppl. 2) (2002) S202–S210.
[12] S. Bortoluzzi, C. Romualdi, A. Bisognin, G.A. Danieli, Disease genes and intracellular protein networks, Physiol. Genomics 15 (2003) 223–227.
[13] J.-D.J. Han, N. Bertin, T. Hao, D.S. Goldberg, G.F. Berriz, L.V. Zhang, D. Dupuy, A.J.M. Walhout, M.E. Cusick, F.P. Roth, M. Vidal, Evidence for dynamically organized modularity in the yeast protein–protein interaction network, Nature 430 (2004) 88–93.
[14] H. Kacser, J.A. Burns, The molecular basis of dominance, Genetics 97 (1981) 639–666.
[15] W.F. Eanes, T.J.S. Merritt, J.M. Flowers, S. Kumagai, E. Sezgin, C.-T. Zhu, Flux control and excess capacity in the enzymes of glycolysis and their relationship to flight metabolism in *Drosophila melanogaster*, Proc. Natl. Acad. Sci. 103 (2006) 19413–19418.
[16] L.M. Raamsdonk, B. Teusink, D. Broadhurst, N. Zhang, A. Hayes, M.C. Walsh, J.A. Berden, K.M. Brindle, D.B. Kell, J.J. Rowland, H.V. Westerhoff, K. van Dam, S.G. Oliver, A functional genomics strategy that uses metabolome data to reveal the phenotype of silent mutations, Nat. Biotechnol. 19 (2001) 45–50.
[17] B. Teusink, J. Passarge, C.A. Reijenga, E. Esgalhado, C.C. van der Weijden, M. Schepper, M.C. Walsh, B.M. Bakker, K. van Dam, H.V. Westerhoff, J.L. Snoep, Can yeast glycolysis be understood in terms of in vitro kinetics of the constituent enzymes? Testing biochemistry, Eur. J. Biochem. 267 (2000) 5313–5329.
[18] R. Heinrich, S. Schuster, The Regulation of Cellular Systems, in: ITP Chapman & Hall, New York, 1996, p. 179.
[19] R. Lagunas, Energy metabolism of *Saccharomyces cerevisiae*: discrepancy between ATP balance and known functions, Biochim. Biophys. Acta 440 (1976) 661–674.
[20] B. Atkinson, F. Mavituna, Biochemical Engineering and Biotechnology Handbook, in: Nature Press, Macmillan Inc., New York, 1983, pp. 120–125.
[21] G. Lidén, A. Persson, C. Niklasson, L. Gustafsson, Energetics and product formation by *Saccharomyces cerevisiae* grown in anaerobic chemostats under nitrogen limitation, Appl. Microbiol. Biotechnol. 43 (1995) 1034–1038.
[22] C. Chapman, W. Bartley, Adenosine phosphates and the control of glycolysis and gluconeogenesis in yeast, Biochem. J. 111 (1969) 609–613.
[23] C. Verduyn, E. Postma, W.A. Schefeers, J. Van-Dijken, Physiology of *Saccharomyces cerevisiae* in anaerobic glucose-limited chemostat cultures, J. Gen. Microbiol. 136 (1990) 395–405.
[24] R.J. Rolfes, Regulation of purine nucleotide biosynthesis: in yeast and beyond, Biochem. Soc. Trans. 34 (2006) 786–790.
[25] S. Gauthier, F. Coulpier, L. Jourdren, M. Merle, S. Beck, M. Konrad, B. Daignan-Fornier, B. Pinson, Co-regulation of yeast purine and phosphate pathways in response to adenylic nucleotide variations, Mol. Microbiol. 68 (2008) 1583–1594.
[26] C. Verduyn, E. Postma, W.A. Scheffers, J.P. Van Dijken, Effect of benzoic acid on metabolic fluxes in yeasts: a continuous-culture study on the regulation of respiration and alcoholic fermentation, Yeast 8 (1992) 501–517.
[27] H.V. Westerhoff, K. Van Dam, Thermodynamics and Control of Biological Free Energy Transduction, Elsevier, Amsterdam, 1987.
[28] U. Theobald, W. Mailinger, M. Baltes, M. Rizzi, M. Reuss, In vivo analysis of metabolic dynamics in Saccharomyces cerevisiae : I. Experimental observations, Biotechnol. Bioeng. 55 (1997) 305–316.
[29] U. Theobald, W. Mailinger, M. Reuss, M. Rizzi, In vivo analysis of glucose-induced fast changes in yeast adenine nucleotide pool applying a rapid sampling technique, Anal. Biochem. 214 (1993) 31–37.
[30] O.J. Somsen, M.A. Hoeben, E. Esgalhado, J.L. Snoep, D. Visser, R.T. van der Heijden, J.J. Heijnen, H.V. Westerhoff, Glucose and the ATP paradox in yeast, Biochem. J. 352 (2000) 593–599.
[31] M. Csete, J. Doyle, Bow ties, metabolism and disease, Trends Biotechnol. 22 (2004) 446–450.
[32] H. Kitano, Biological robustness, Nat. Rev. Genet. 5 (2004) 826–837.
[33] H.V. Westerhoff, C. Winder, H. Messiha, E. Simeonidis, M. Adamczyk, M. Verma, F.J. Bruggeman, W. Dunn, Systems biology: the elements and principles of Life, FEBS Lett. 583 (2009) 3882–3890.
[34] H. Lehrach, R. Subrak, P. Boyle, M. Pasterk, K. Zatloukal, H. Müller, T. Hubbard, A. Brand, M. Girolami, D. Jameson, F.J. Bruggeman, H.V. Westerhoff, ITFoM—the IT future of medicine, Proc. Comput. Sci. 7 (2011) 27–29.
[35] M. Rizzi, M. Baltes, U. Theobald, M. Reuss, In vivo analysis of metabolic dynamics in Saccharomyces cerevisiae: II. Mathematical model, Biotechnol. Bioeng. 55 (1997) 592–608.
[36] F. Schaedel, E. Franco-Lara, Rapid sampling devices for metabolic engineering applications, Appl. Microbiol. Biotechnol. 83 (2009) 199–208.
[37] A. Canelas, C. Ras, A. ten Pierick, J. van Dam, J. Heijnen, W. van Gulik, Leakage-free rapid quenching technique for yeast metabolomics, Metabolomics 4 (2008) 226–239.
[38] O. Vielhauer, M. Zakhartsev, T. Horn, R. Takors, M. Reuss, Simplified absolute metabolite quantification by gas chromatography–isotope dilution mass spectrometry on the basis of commercially available source material, J. Chromatogr. B 879 (2011) 3859–3870.
[39] S.G. Villas-Bôas, J. Højer-Pedersen, M. Åkesson, J. Smedsgaard, J. Nielsen, Global metabolite analysis of yeast: evaluation of sample preparation methods, Yeast 22 (2005) 1155–1169.
[40] M.R. Mashego, L. Wu, J.C. Van Dam, C. Ras, J.L. Vinke, W.A. Van Winden, W.M. Van Gulik, J.J. Heijnen, MIRACLE: mass isotopomer ratio analysis of U-13C-labeled extracts. A new method for accurate quantification of changes in concentrations of intracellular metabolites, Biotechnol. Bioeng. 85 (2004) 620–628.

[41] S. Buziol, I. Bashir, A. Baumeister, W. Claaßen, N. Noisommit-Rizzi, W. Mailinger, M. Reuss, New bioreactor-coupled rapid stopped-flow sampling technique for measurements of metabolite dynamics on a subsecond time scale, Biotechnol. Bioeng. 80 (2002) 632–636.
[42] M.T.A.P. Kresnowati, W.A. van Winden, M.J.H. Almering, A. ten Pierick, C. Ras, T.A. Knijnenburg, P. Daran-Lapujade, J.T. Pronk, J.J. Heijnen, J.M. Daran, When transcriptome meets metabolome: fast cellular responses of yeast to sudden relief of glucose limitation, Mol. Syst. Biol. 2 (2006) (Article number: 49).
[43] M.O. Loret, L. Pedersen, J. François, Revised procedures for yeast metabolites extraction: application to a glucose pulse to carbon-limited yeast cultures, which reveals a transient activation of the purine salvage pathway, Yeast 24 (2007) 47–60.